INSTITUTE OF PHYSICS PUBLISHING JOURNAL OF PHYSICS B: ATOMIC, MOLECULAR AND OPTICAL PHYSICS

J. Phys. B: At. Mol. Opt. Phys. **36** (2003) 3281–3291 PII: S0953-4075(03)63439-5

# Hyperspherical close-coupling calculations for charge transfer cross sections in $Si^{4+}$ + H(D) and $Be^{4+}$ + H collisions at low energies

**Anh-Thu Le, Michel Hesse, T G Lee and C D Lin**

Department of Physics, Cardwell Hall, Kansas State University, Manhattan, KS 66506, USA

Received 13 May 2003, in final form 10 June 2003
Published 15 July 2003
Online at stacks.iop.org/JPhysB/36/3281

**Abstract**

Total and partial electron capture cross sections are calculated for $Si^{4+}$ + H(1s)/D(1s) collisions from 1 meV amu$^{-1}$ to 1 keV amu$^{-1}$, and for $Be^{4+}$ + H(1s) collisions from 2.5 eV amu$^{-1}$ up to 1 keV amu$^{-1}$, using the recently developed hyperspherical close-coupling (HSCC) approach. For both systems, our results are in good agreement with calculations based on the molecular orbital expansion method in reaction coordinates (RC). For $Si^{4+}$ + D(1s) our total charge transfer cross sections agree well with experiment, but not the partial cross sections. For $Be^{4+}$ + H, we show that partial wave cross sections from the RC method have more oscillatory structures than those from the HSCC method, even though the total cross sections agree. In comparison with the RC method, the HSCC approach does not require the introduction of any *ad hoc* external parameters in the formulation.

(Some figures in this article are in colour only in the electronic version)

## 1. Introduction

In a recent paper a hyperspherical close-coupling (HSCC) method has been developed to study ion–atom collisions at low energies [1]. This method has been used to analyse charge transfer cross sections in $He^{2+}$ + H collisions [1] and in $H^+$ + Na collisions [2]. For ion–atom collisions at low energies, the traditional standard theoretical approach is the perturbed stationary states (PSS) approximation, where the total wavefunction is expanded in terms of molecular orbitals of the transient molecule. The PSS method is known to have many fundamental difficulties [3]. Remedies to the PSS method include the introduction of switching functions or the adoption of the so-called reaction coordinates (RC). While both approaches have been very successful in predicting cross sections in good agreement with experiments, both the switching functions and the RC have to be chosen with some auxiliary external conditions. While calculations based on the HSCC method have been carried out for $He^{2+}$ + H and $H^+$ + Na systems, there

  

are no reliable experimental data for comparison at low energies, and comparison with other calculations can only be made for the total cross sections.

In this paper, we present the HSCC results for two collision systems: $Si^{4+} + H(D)$ and $Be^{4+} + H$. The RC method has been applied to both systems. For $Si^{4+} + D$ collisions, the total electron capture cross section has been measured by Pieksma *et al* [4] in a merged beam experiment for collision energies down to about 0.01 eV amu$^{-1}$. At such low energies, calculations using the RC method [4, 5] showed the presence of a large isotope effect, i.e., the cross section for the $Si^{4+} + D$ collision is different from the one for the $Si^{4+} + H$ collision at the same velocity. Furthermore, at low energies the total electron capture cross sections appear to display the Langevin limit, i.e., the cross section increases as $1/v$, where $v$ is the relative collision velocity. We employed the HSCC method to study this system in view of the existence of experimental data down to about 0.01 eV amu$^{-1}$ and the availability of calculations based on the RC method. For the $Be^{4+} + H(1s)$ collision, careful study has been made by Errea *et al* [6, 7] in the energy region 2.5 eV amu$^{-1}$–25 keV amu$^{-1}$. Two approaches have been used: a semi-classical treatment modified with a common translation factor [8], and a quantum mechanical treatment modified with a common reaction coordinate (CRC) [9, 10]. Both methods employ some form of switching function whose origin lies in the semi-classical approach. Their semi-classical treatment is well adapted to the high energy region which has been widely studied, at least theoretically [11–15]. Our focus will be in the lower energy region where the work of Errea *et al* [6, 7] is the only known theoretical calculation available. An added advantage of this system is that partial wave cross sections have been presented by Errea *et al* [7] at a few energies, thus allowing us to compare the partial wave cross sections with those from the HSCC method.

The recently developed HSCC method for ion–atom collisions is based on the standard HSCC method for treating general three-body collision systems [16], but specifically modified for collisions involving two heavy nuclei and one light electron. This method provides a full quantum mechanical treatment of the collision without any *ad hoc* parameters. Its validity would be judged by the rate of convergence of the number of channels included in the calculation. By comparing the results of the HSCC method we aim to establish the validity of the HSCC method, and also the validity of the RC method.

In section 2, we review briefly the HSCC method for ion–atom collisions. Results for $Si^{4+} + H(D)$ and for $Be^{4+} + H(1s)$ reactions are presented in section 3. A summary and conclusions are given in section 4. Atomic units are used unless otherwise indicated.

## 2. The hyperspherical close-coupling method

To determine electron capture cross sections, say, in $Be^{4+} + H(1s)$ collisions, we use the HSCC method. In combination with the $R$-matrix propagation method and slow/smooth-variable discretization techniques, the HSCC approach has been described in detail in [1]. Here we summarize only the essentials of the method.

The three particles in $BeH^{4+}$ are described with the help of mass-weighted hyperspherical coordinates. In the 'molecular' frame, the first Jacobi vector $\boldsymbol{\rho}_1$ is chosen to be the vector from $Be^{4+}$ to $H^+$, with reduced mass $\mu_1$. The second Jacobi vector $\boldsymbol{\rho}_2$ goes from the centre of mass of $Be^{4+}$ and $H^+$ to the electron, with reduced mass $\mu_2$. The hyperradius $R$ and hyperangle $\phi$ are defined as

$$R = \sqrt{\frac{\mu_1}{\mu}\rho_1^2 + \frac{\mu_2}{\mu}\rho_2^2}. \tag{1}$$

$$\tan\phi = \sqrt{\frac{\mu_2}{\mu_1}}\frac{\rho_2}{\rho_1} \tag{2}$$

where $\mu$ is arbitrary. Another angle, $\theta$, is defined as the angle between the two Jacobi vectors. When $\mu$ is chosen equal to $\mu_1$, the hyperradius $R$ becomes very close to the internuclear distance for an ion–atom collision system.

After introducing the rescaled wavefunction

$$\Psi(R, \Omega, \hat{\omega}) = \psi(R, \Omega, \hat{\omega}) R^{3/2} \sin\phi\cos\phi, \tag{3}$$

the Schrödinger equation takes the form

$$\left(-\frac{1}{2}\frac{\partial}{\partial R}R^2\frac{\partial}{\partial R} + \frac{15}{8} + H_{\rm ad}(R, \Omega, \hat{\omega}) - \mu R^2 E\right)\Psi(R, \Omega, \hat{\omega}) = 0, \tag{4}$$

where $\Omega \equiv \{\phi, \theta\}$, and $\hat{\omega}$ denotes the three Euler angles of the body-fixed frame with respect to the space-fixed frame. $H_{\rm ad}$ is the adiabatic Hamiltonian

$$H_{\rm ad}(R, \Omega, \hat{\omega}) = \frac{\Lambda^2}{2} + \mu R C(\Omega), \tag{5}$$

where $\Lambda^2$ is the grand-angular momentum operator and $C(\Omega)/R$ gives the total Coulomb interaction.

To solve equation (4), we expand the rescaled wavefunction in terms of normalized and symmetrized rotation functions $\tilde{D}$, and body-frame adiabatic basis functions $\Phi_{\mu I}(R, \Omega)$

$$\Psi(R, \Omega, \hat{\omega}) = \sum_{\nu}\sum_{I} F_{\nu I}(R)\Phi_{\nu I}(R, \Omega)\tilde{D}^J_{IM_J}(\hat{\omega}) \tag{6}$$

where $\nu$ is the channel index, $J$ is the total angular momentum, $I$ is the absolute value of the projection of $\boldsymbol{J}$ along the body-fixed $z'$ axis and $M_J$ is the projection along the space-fixed $z$ axis. To solve the hyperradial equations we divide the hyperradial space into sectors. We then use a combination of the $R$-matrix propagation method [17] to propagate the $R$-matrix from one sector to the next, and a slow/smooth-variable discretization method [18] within each sector. The $R$-matrix is propagated to a large hyperradius (depending on the collision energy) where the solution is matched to the known asymptotic solutions to extract the scattering matrix. The electron capture cross section for each partial wave $J$ is then obtained from the calculated scattering matrix.

The method described above has to be carried out for each partial wave $J$ until a converged cross section is reached. Using the numerical procedure introduced in Liu *et al* [1] such calculations can be easily carried out for many partial waves. We have checked that the results are insensitive to the matching radius within the number of channels included in the calculation, see below.

To apply the HSCC method to $Si^{4+}$ + H(D), we treat $Si^{4+}$ as an inert ionic core described by a model potential. The model potential is taken from the early work of Gargaud and McCarroll [5]. Thus the starting approximate Hamiltonian is the same and any differences from the HSCC method and the RC method are due to the dynamic treatment of the collision system.

## 3. Results

### *3.1. $Si^{4+}$ + H(D) collisions*

The hyperspherical potential curves used in the present calculation for the $Si^{4+}$ + H system are shown in figure 1. Each curve is labelled by its asymptotic limit and only $I = 0$ and 1

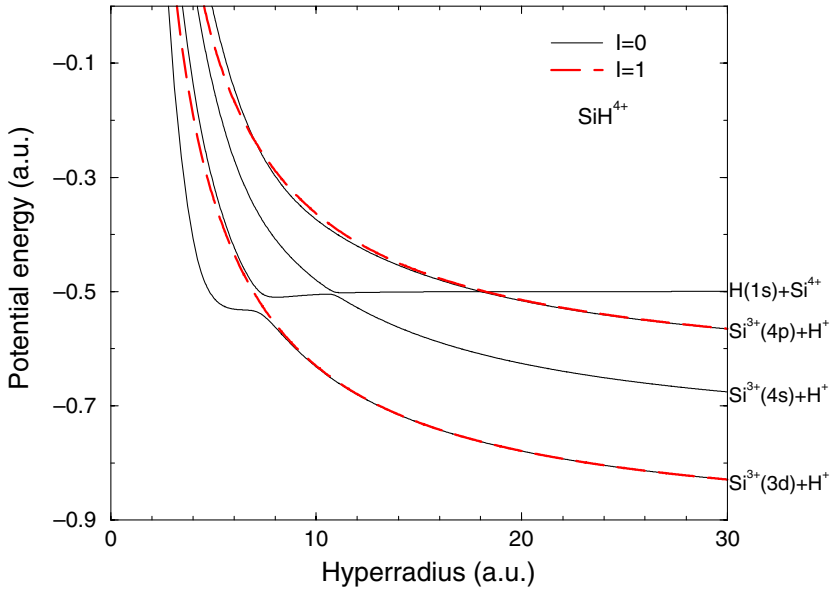


**Figure 1.** Hyperspherical adiabatic potential curves for $SiH^{4+}$. The figure shows four $I = 0$ channels (solid curves) and two $I = 1$ channels (broken curves).

are included. The sharp avoided crossing between the entrance channel $Si^{4+} + H$ and the $Si^{3+}(4p) + H^+$ at $R$ near 18 au is very narrow. This crossing was treated as completely diabatic in [5]. We did not make such an approximation but our calculation indeed shows that this crossing is diabatic down to the 1 meV $amu^{-1}$ studied here. From the calculations, the major transitions occur at the avoided crossing near $R = 11$ au, which would populate the $Si^{3+}(4s)$ state at the end of the collision, and at the avoided crossing near $R = 7.5$ au which would populate the $Si^{3+}(3d)$ state. The $Si^{3+}(4s)$ state is predominantly populated at low collision energies while $Si^{3+}(3d)$ is populated at higher energies. Note that the potential curves in figure 1 are essentially identical to the Born–Oppenheimer potential curves used in Gargaud and McCarroll [5]. We have calculated the hyperspherical potential curves for $Si^{4+} + H$ and $Si^{4+} + D$ systems separately. At the accuracy shown in the figure, they are indistinguishable.

In figure 2 we show the total charge transfer cross sections for $Si^{4+} + H(D)$ collisions versus collision energies from 1 meV $amu^{-1}$ to 1 keV $amu^{-1}$. We compare our results with the experimental data and theoretical calculations given in [4]. Our results are in good agreement with the theoretical results reported in that paper where the cross sections were carried out using the RC method as described in [5]. The small differences among the theories are mostly due to the fact that the calculations were being carried out at different energies. Thus, using the same Hamiltonian, the HSCC and the RC method gave essentially identical total charge transfer cross sections and the results are in good agreement with experiment.

Partial electron capture cross sections in general are difficult to obtain from the merged beam experiments. Despite this, Wu and Havener [19] have been able to extract the ratio of electron capture cross sections to 3d with respect to 4s for $Si^{4+} + D$ collisions. Their results for this ratio are 1.3 and 1.8 for collisions at 50.6 and 98.6 eV $amu^{-1}$, respectively, which should be compared to 2.3 and 3.2 from the calculations of Gargaud and McCarroll [5] and 2.1 and 2.8 from the present HSCC calculations. In other words, the two theoretical results agree with each other, but not with experiment.

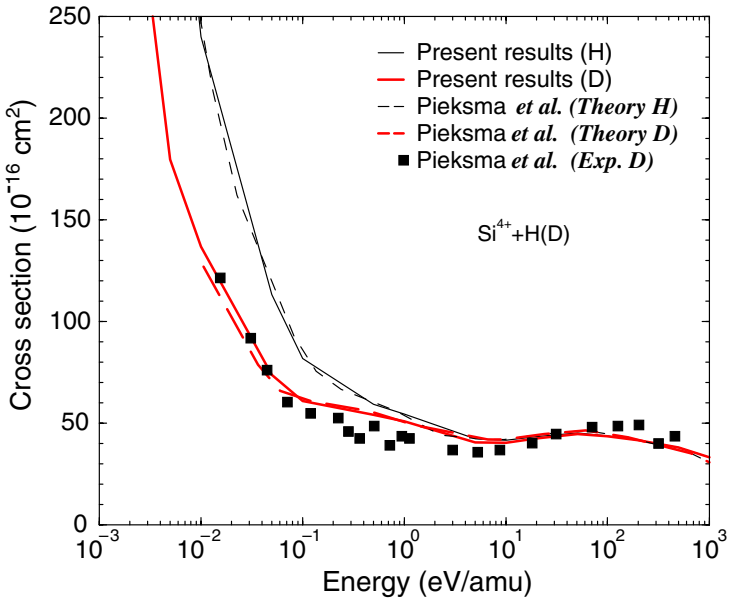


**Figure 2.** Comparison of the total charge transfer cross sections from our calculations and Pieksma *et al* [4] for $Si^{4+}$ colliding with H or D. Solid curves correspond to our results. Broken curves and squares correspond to the theoretical and experimental results of Pieksma *et al*, respectively. In the electronic version the results for H(D) are given by black (red) curves.

The experimental data of Pieksma *et al* and the theoretical calculations indicate that the total charge transfer cross sections for $Si^{4+}$ + D(H) appear to follow the Langevin model for collision energies below 0.1 eV amu$^{-1}$. The validity of a classical model for predicting charge transfer cross sections at such small collision energies seems intriguing. According to the Langevin model, for each collision energy $E$ there is a critical impact parameter $b_c$ such that for $b < b_c$ the incident particle can overcome the effective potential barrier and become trapped by the inner potential well where electron capture can occur. We examine if the quantum calculations support this classical prediction. For this purpose, we employ the relation:

$$\sigma_J = \frac{2\pi b P(b)}{k}, \tag{7}$$

with $J = kb$, where $k$ is the momentum, to extract the electron capture probability from each calculated partial wave cross section. In figure 3 we show $P(b)$ versus $b$ for total electron capture probabilities at three different energies. Clearly the range of impact parameters for electron capture increases with decreasing energies. The value of $b_c$ for each energy according to the Langevin model is also indicated. Assuming that the probability for electron capture is one half for $0 < b < b_c$, we calculated the total electron capture cross section according to the Langevin model to be 1000, 1414 and 3167 au, which are to be compared to the values of 857, 1466 and 3772 au obtained from the quantum calculations for $E = 10$, 5 and 1 meV amu$^{-1}$, respectively. The cutoff impact parameters from the Langevin model for the three energies are 25.2, 30.0 and 44.9 au, are also in good agreement with the cutoff from the quantum calculations, indicating that tunnelling does not contribute significantly to the total charge transfer cross sections.

The results of figure 2 also show a significant isotope effect for collision energies below 1 eV amu$^{-1}$. According to a molecular approach such as the RC method, the Born–

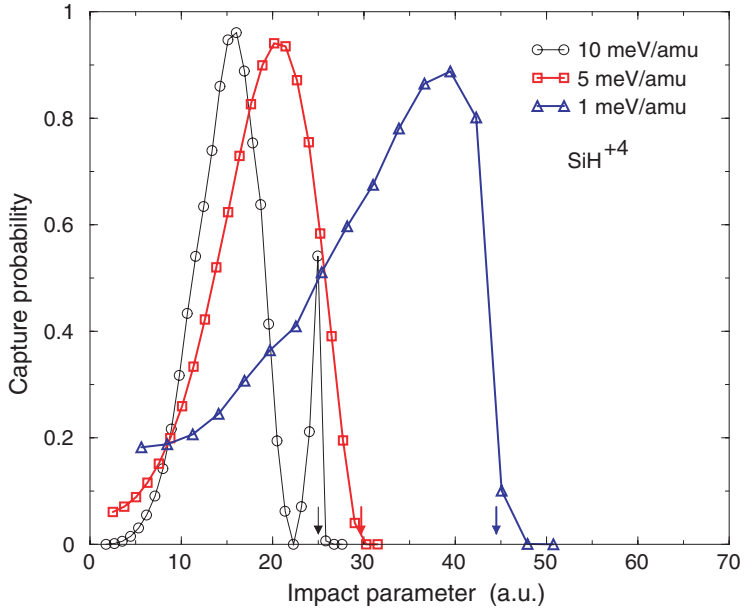


**Figure 3.** Electron capture probabilities versus impact parameters at low energies. The arrows indicate the values of the critical impact parameter $b_c$, according to the Langevin model, where the incident ion can overcome the effective centrifugal potential barrier of the ion–atom collision system.

Oppenheimer potential curves are independent of the mass of the heavy particles. Thus the isotope effect comes entirely from the different effective mass in the radial equation. In the HSCC method, the hyperspherical potential curves depend on the mass of each nucleus. In principle, one can expect the isotope effect to also come from the different potential curves. For the present systems in the meV amu$^{-1}$ energy region, however, we found that such an effect is negligible.

### 3.2. $Be^{4+} + H$ collisions

We next consider electron capture cross sections for the reaction

$$\mathrm{Be}^{4+} + \mathrm{H}(1\mathrm{s}) \rightarrow \mathrm{Be}^{3+}(n) + \mathrm{H}^{+}. \tag{8}$$

To compare the present HSCC method with the CRC method used by Errea *et al* [6, 7] we used the same set of molecular orbitals (or hyperspherical channels) in the calculation. The adiabatic hyperspherical potentials including the incident channel and those leading to the capture into $\mathrm{Be}^{3+}(n = 3, 4)$ states are shown in figure 4. For clarity, only the $I = 0$ and 1 components are shown. (The inset shows the close-up of the entrance channel with two other channels near the avoided crossing region.) In the actual calculations all the $I = 0$, 1, 2 and 3 components have been included, the same as in the calculations of Errea *et al*, even though the $I = 2$ and 3 components make only small contributions.

In table 1 the total and partial cross sections to the $n = 3$ and 4 states of $\mathrm{Be}^{3+}$ are tabulated against the results from Errea *et al*. To begin with, we note that the total cross sections from the two calculations agree very well over the whole velocity range. Since electron capture to the $n = 3$ states of $\mathrm{Be}^{3+}$ is dominant, the agreement for the $n = 3$ partial cross sections is also

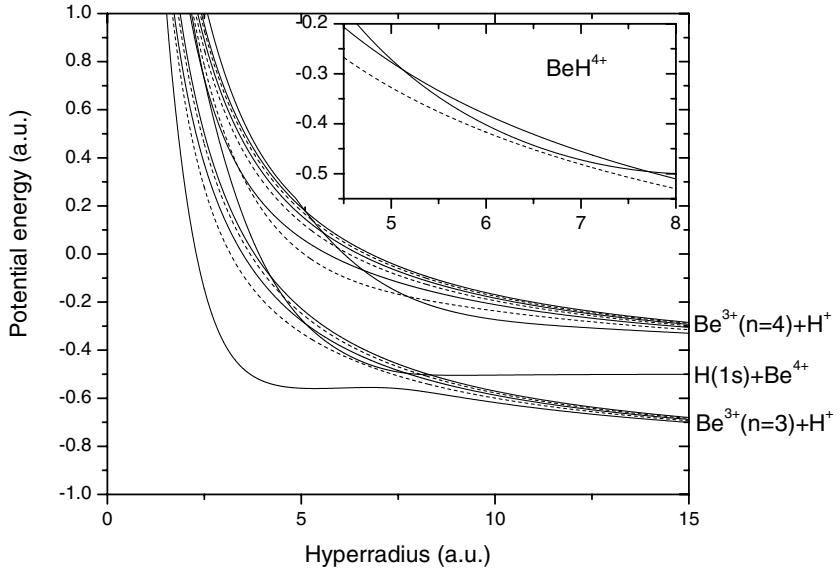


**Figure 4.** Hyperspherical adiabatic potential curves $U_\mu^I$ for $BeH^{3+}$, corresponding to $n = 3$ and 4 manifolds, and to the entrance channel. Only eight $I = 0$ channels and five $I = 1$ channels are shown. The inset gives a close-up view of the three potential curves near the avoided crossing region at $R$ near 5 au.

**Table 1.** Partial and total electron capture cross sections in units of $10^{-16}$ $cm^2$ for $Be^{4+}$ + H(1s) collisions with a collision velocity smaller than 0.2 au. The first line for each velocity corresponds to our results, and the second line to the quantum mechanical (Q17) or semi-classical (S96) results of Errea *et al* [7].

| $v$ (au) | | $n = 3$ | $n = 4$ | Total |
|---|---|---|---|---|
| 0.01 | | 0.40 | 0 | 0.40 |
| | Q17 | 0.42 | 0 | 0.42 |
| 0.02 | | 2.41 | 0.002 | 2.41 |
| | Q17 | 2.42 | 0.018 | 2.44 |
| 0.03 | | 5.23 | 0.005 | 5.23 |
| | Q17 | 5.28 | 0.05 | 5.34 |
| 0.04 | | 8.49 | 0.22 | 8.71 |
| | Q17 | | | |
| 0.05 | | 11.84 | 0.66 | 12.50 |
| | Q17 | 11.87 | 0.64 | 12.51 |
| 0.07 | | 17.72 | 1.78 | 19.50 |
| | Q17 | 17.92 | 1.92 | 19.85 |
| 0.1 | | 24.07 | 2.78 | 26.85 |
| | Q17 | 24.51 | 2.94 | 27.46 |
| 0.2 | | 32.53 | 3.09 | 35.62 |
| | S96 | 34.42 | 3.11 | 37.61 |

very good. For the weaker $n = 4$ channels, results show very good agreement for $v = 0.2$ down to 0.05 au. For $v = 0.03$ and 0.02 au, our $n = 4$ partial cross sections are much smaller than the results quoted in Errea *et al*.

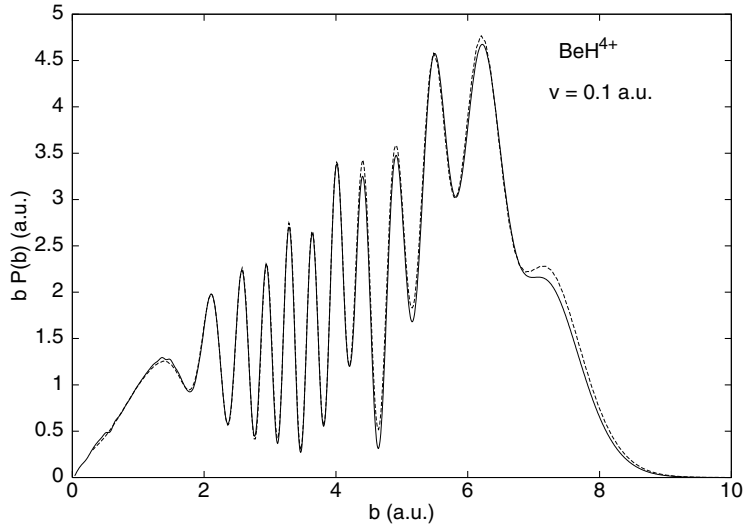


**Figure 5.** Total charge transfer transition probability $P(b)$ times impact parameter $b$ as a function of $b$ at $v = 0.1$ au. The solid and broken curves correspond to our quantum mechanical calculations and to the results of [7], respectively.

The precise reason for the discrepancy in $n = 4$ channels is somewhat complicated. In the approach of Errea *et al*, the potential curves are identical to the Born–Oppenheimer potential curves. For a one-electron, two-nuclei Coulomb system at a fixed internuclear distance, the Hamiltonian is separable in the BO approach such that potential curves of the same symmetry can cross. This is not the case for the HSCC approach with the hyperradius being the adiabatic parameter. Thus the real crossing in the BO potential curves becomes the sharp avoided crossing in the HSCC approach. Therefore, even if the same number of channels are used in the calculation, the two approaches do not include the same channels in the region of small hyperradius or internuclear distance. To remedy this situation the data for the $n = 4$ channels shown in table 1 at low energies were calculated by including some channels that dissociate to the $Be^{3+}(n = 5)$ states. These higher adiabatic channels incorporate part of the diabatic $Be^{3+}(n = 4)$ states at the small internuclear distances of Errea *et al*. (To use exactly the same channels we would need to obtain diabatic hyperspherical channels for states involved in the avoided crossing—a project in progress.) On the other hand, we have no reason to believe that the HSCC and the RC results have to agree with each other at low energies for the small channels. Such discrepancies have been observed in $He^{2+} + H$ collisions [1] and in protons colliding with Na [2] at low energies. It was shown in Le *et al* [2] that the coupling matrix elements from RC and the HSCC are not identical. From the HSCC viewpoint, the accuracy of the $n = 4$ channels can be checked by increasing the base size if accurate cross sections are needed.

One of the main goals of the present study is to compare in detail the results from the HSCC with those from the CRC. For this purpose, we compare the partial wave cross sections at three different energies in figures 5–7. (The CRC results were kindly provided by Dr Luis Mendez.) In figure 5, we compare the two calculations at $v = 0.1$ au, showing the impact parameter weighted probability $bP(b)$ for the total electron capture processes. Note that the two calculations show amazingly good agreement in detail. In figure 6 we compare the same weighted probabilities for $v = 0.05$ au. The agreement is again very good, especially at large

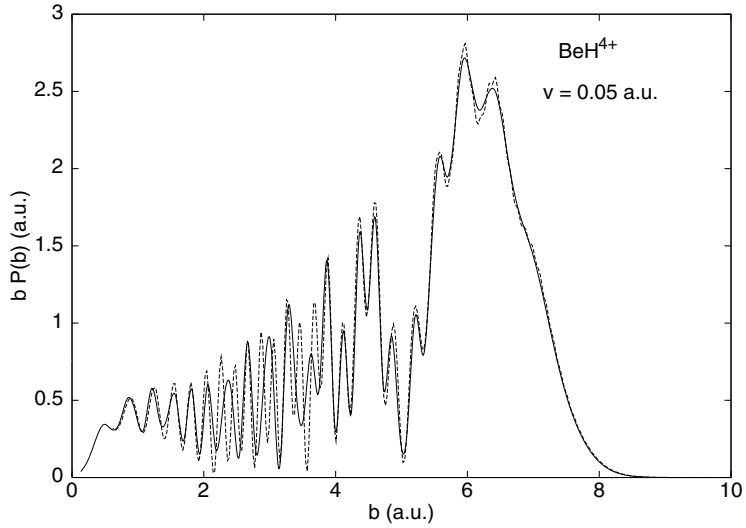


**Figure 6.** Total charge transfer transition probability $P(b)$ times impact parameter $b$ as a function of $b$ at $v = 0.05$ au. The solid and broken curves correspond to our quantum mechanical calculations and to the results of [7], respectively.

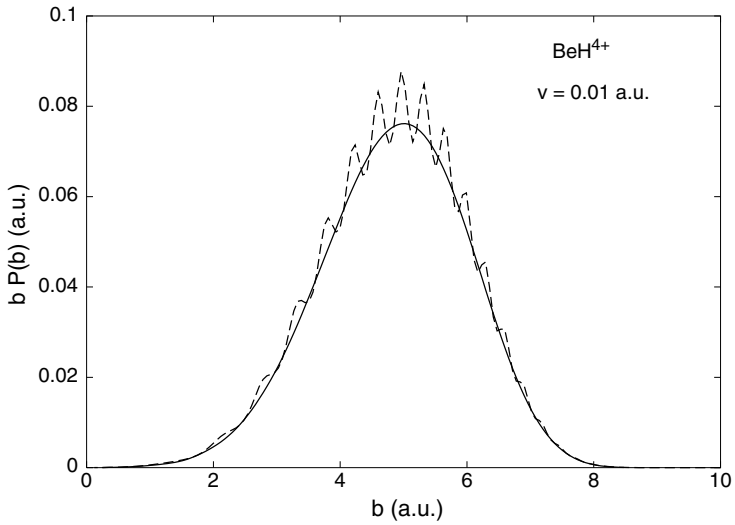


**Figure 7.** Total charge transfer transition probability $P(b)$ times impact parameter $b$ as a function of $b$ at $v = 0.01$ au. The solid and broken curves correspond to our quantum mechanical calculations and to the results of [7], respectively.

and small impact parameters. There are deviations for $b$ ranging from 2 to 4 au with the CRC calculations showing more oscillations than from the HSCC calculations. At $v = 0.01$ au, as shown in figure 7, the overall agreement is still very good, but the CRC results present more oscillatory structures on top of the smooth curve from the HSCC calculations.

From the results shown above it is clear that the calculations based on the CRC and the HSCC methods are very close to each other in the larger features, particularly for the dominant

channels. The CRC method as implemented by Errea *et al* expands the total wavefunction similar to equation (6) except that the hyperradius is replaced by a RC $\boldsymbol{\xi}$, and the channel functions were solved by fixing $\xi = \rho$, where $\rho$ is the internuclear separation. The RC $\boldsymbol{\xi}$ is expressed in the form

$$\boldsymbol{\xi} = \boldsymbol{\rho} + \boldsymbol{s}(\boldsymbol{r}, \boldsymbol{\rho})/\mu \tag{9}$$

where $\boldsymbol{s}(\boldsymbol{r}, \boldsymbol{\rho})$ is defined by

$$\boldsymbol{s}(\boldsymbol{r}, \boldsymbol{\rho}) = f(r, \rho)\boldsymbol{r} - \tfrac{1}{2} f^2(r, \rho)\boldsymbol{\rho} \tag{10}$$

and where $f(r, \rho)$ is the switching function and $\boldsymbol{r}$ is the electronic coordinate. The switching function $f$ has been chosen such that the asymptotic boundary conditions are correctly represented, thus ensuring that the resulting equations are Galilean invariant. The choice of $f$ is decided based on the physical model for collisions at higher velocities, i.e., from the semiclassical regime [6, 20].

A causal look at the HSCC and the CRC methods would prompt one to speculate that the RC plays, to some extent, a role similar to the hyperradius in the HSCC method. The fact that calculations from the two methods agree so well over the velocity range covered seems to indicate that the CRC method can be used to describe ion–atom collisions at low energies despite the fact that the switching function is not uniquely defined, i.e., the results appear to be insensitive to the precise form of the switching function chosen. On the other hand, the remaining discrepancy between the HSCC and the CRC method may indicate the degree of inaccuracy introduced by the *ad hoc* switching functions in the latter model. Since the HSCC method does not introduce any approximations at the beginning, and adiabatic channel functions are used in the expansion, one would expect that the convergence of HSCC is better at lower energies. Thus we would tend to attribute the presence of extra oscillatory structures in the partial wave total charge transfer cross sections to the result of the use of the switching functions, as seen in figures 6 and 7.

## 4. Summary and conclusions

In this paper we used the HSCC method to calculate electron capture cross sections for $Si^{4+}$ + H(D) and $Be^{4+}$ + H(1s) collisions from about 1 meV amu$^{-1}$ up to 1 keV amu$^{-1}$. For $Si^{4+}$ + H(D) the total electron transfer cross sections are found to be in good agreement with the experimental data and theoretical calculations in Pieksma *et al* [4]. For $Be^{4+}$ + H, we found that the total charge transfer cross sections are in good agreement with the CRC method of Errea *et al* [6, 7]. We did find some discrepancies in the cross sections for electron capture to the weaker $n = 4$ manifold, as well as in the partial wave cross sections at low energies. The agreement between the CRC and the HSCC method indicates that both approaches are capable of describing low energy ion–atom collisions. The advantage of the HSCC method is that it introduces no *ad hoc* parameters in the formulation. We have also compared the HSCC and the CRC results at the level of partial wave cross sections or the equivalent impact parameter probabilities. At $v = 0.1$ au we found perfect agreement. Slight deviations occur at lower velocities where the CRC results show more oscillations than the HSCC method. Similarly, for the total electron capture cross sections to the weaker $n = 4$ channels we found discrepancies between the two calculations at low energies.

The general agreement between the CRC and the HSCC method is encouraging. Since the HSCC method is so far limited to one-electron collision systems, while the CRC method has been applied to many-electron systems, the good agreement in the two calculations implies that the CRC calculations for complex systems can be expected to be adequate as well. Finally the general agreement between the CRC and the HSCC method probably comes from an

equivalence between the hyperradius and the RC used in the literature, at least to first order in the mass ratio of the electron to that of the mass of the heavy particles. This issue remains to be addressed in the future.

## Acknowledgment

This work was supported in part by Chemical Sciences, Geosciences and Biosciences Division, Office of Basic Energy Sciences, Office of Science, US Department of Energy.

## References

[1] Liu C-N, Le A-T, Morishita T, Esry B D and Lin C D 2003 *Phys. Rev.* A **67** 052705
[2] Le A-T, Liu C-N and Lin C D 2003 *Phys. Rev.* A at press
[3] Delos J B 1981 *Rev. Mod. Phys.* **53** 287
[4] Pieksma M, Gargaud M, McCarroll R and Havener C C 1996 *Phys. Rev.* A **54** R13
[5] Gargaud M and McCarroll R 1988 *J. Phys. B: At. Mol. Opt. Phys.* **21** 513
[6] Errea L F, Gorfinkiel J D, Harel C, Jouin H, Macías A, Méndez L, Pons B and Riera A 1996 *Phys. Scr.* T **62** 33
[7] Errea L F, Harel C, Jouin H, Méndez L, Pons B and Riera A 1998 *J. Phys. B: At. Mol. Opt. Phys.* **31** 3527
[8] Schneiderman S B and Russek A 1969 *Phys. Rev.* **181** 311
[9] Mittleman M H 1969 *Phys. Rev.* **188** 221
[10] Thorson W R and Delos J B 1978 *Phys. Rev.* A **18** 135
[11] Errea L F, Méndez L and Riera A 1982 *Phys. Lett.* A **92** 231
[12] Kimura M and Thorson W R 1983 *J. Phys. B: At. Mol. Phys.* **16** 1471
[13] Fritsch W and Lin C D 1984 *Phys. Rev.* A **29** 3039
[14] Janev R K, Solov'ev E A and Ivanovski G 1996 *Phys. Scr.* T **62** 43
[15] Schultz D R, Krstić P S and Reinhold C O 1996 *Phys. Scr.* T **62** 69
[16] Lin C D 1995 *Phys. Rep.* **257** 1
[17] Baluja K L, Burke P G and Morgan L A 1982 *Comput. Phys. Commun.* **27** 299
[18] Tolstikhin O I, Watanabe S and Matsuzawa M 1996 *J. Phys. B: At. Mol. Opt. Phys.* **29** L389
[19] Wu W and Havener C C 1997 *J. Phys. B: At. Mol. Opt. Phys.* **30** L213
[20] Harel C and Jouin H 1990 *J. Phys. B: At. Mol. Opt. Phys.* **24** 3219
Harel C and Jouin H 1990 *Europhys. Lett.* **11** 121